

Encapsulation efficiency of CdSe/ZnS quantum dots by liposomes determined by thermal lens microscopy

Jessica Batalla,¹ Humberto Cabrera,^{2,3,*} Eduardo San Martín-Martínez,¹ Dorota Korte,⁴ Antonio Calderón¹ and Ernesto Marín¹

¹Instituto Politécnico Nacional, Centro de Investigación en Ciencia Aplicada y Tecnología Avanzada, Unidad Legaria, México D.F. 11500, Mexico

²SPIE-ICTP Anchor Research Laboratory, International Centre for Theoretical Physics (ICTP), Strada Costiera 11, Trieste 34151, Italy

³Centro Multidisciplinario de Ciencias, Instituto Venezolano de Investigaciones Científicas (IVIC), Mérida 5101, Venezuela

⁴Laboratory for Environmental Research, University of Nova Gorica, Vipavska 13, 5000 Nova Gorica, Slovenia
*hcabrera@ictp.it

Abstract: In this study the encapsulation of core shell carboxyl CdSe/ZnS quantum dots (QDs) by phospholipids liposome complexes is presented. It makes the quantum dots water soluble and photo-stable. Fluorescence self-quenching of the QDs inside the liposomes was observed. Therefore, the thermal lens microscopy (TLM) was found to be an useful tool for measuring the encapsulation efficiency of the QDs by the liposomes, for which an optimum value of 36% was determined. The obtained limit of detection (LOD) for determining QDs concentration by TLM was 0.13 nM. Moreover, the encapsulated QDs showed no prominent cytotoxicity toward Breast cancer cells line MDA-MB-231. This study was supported by UV-visible spectroscopy, high resolution transmission electron microscopy (HRTEM) and dynamic light scattering measurements (DLS).

©2015 Optical Society of America

OCIS codes: (170.0180) Microscopy; (170.0110) Imaging systems; (350.6830) Thermal lensing; (170.3880) Medical and biological imaging; (170.1530) Cell analysis

References and links

1. N. Sounderya and Y. Zhang, "Use of core/shell structured nanoparticles for biomedical applications," *Recent Pat. Biomed. Eng.* **1**(1), 34–42 (2008).
2. M. K. So, H. Yao, and J. Rao, "Halo tag protein-mediated specific labeling of living cells with quantum dots," *Biochem. Biophys. Res. Commun.* **374**(3), 419–423 (2008).
3. A. M. Derfus, W. C. W. Chan, and S. N. Bhatia, "Probing the cytotoxicity of semiconductor quantum dots," *Nano Lett.* **4**(1), 11–18 (2004).
4. G. D. Bothun, A. E. Rabideau, and M. A. Stoner, "Hepatoma cell uptake of cationic multifluorescent quantum dot liposomes," *J. Phys. Chem. B* **113**(22), 7725–7728 (2009).
5. D. R. Larson, W. R. Zipfel, R. M. Williams, S. W. Clark, M. P. Bruchez, F. W. Wise, and W. W. Webb, "Water-soluble quantum dots for multiphoton fluorescence imaging in vivo," *Science* **300**(5624), 1434–1436 (2003).
6. K. Susumu, B. C. Mei, and H. Mattoussi, "Multifunctional ligands based on dihydrolipoic acid and polyethylene glycol to promote biocompatibility of quantum dots," *Nat. Protoc.* **4**(3), 424–436 (2009).
7. A. M. Smith, H. Duan, M. N. Rhyner, G. Ruan, and S. Nie, "A systematic examination of surface coatings on the optical and chemical properties of semiconductor quantum dots," *Phys. Chem. Chem. Phys.* **8**(33), 3895–3903 (2006).
8. L. Spanhel, L. M. Haase, H. Weller, and A. Henglein, "Photochemistry of colloidal semiconductors. Surface modification and stability of strong luminescing CdS particles," *J. Am. Chem. Soc.* **109**(19), 5649–5655 (1987).
9. W. Zou, Z. J. Du, H. Q. Li, and C. Zhang, "Fabrication of carboxyl functionalized CdSe quantum dots via ligands self-assembly and CdSe/epoxy fluorescence nanocomposites," *Polymer (Guildf.)* **52**(9), 1938–1943 (2011).
10. G. Kalyuzhny and R. W. Murray, "Ligand effects on optical properties of CdSe nanocrystals," *J. Phys. Chem. B* **109**(15), 7012–7021 (2005).
11. M. Kuno, J. K. Lee, B. O. Dabbousi, F. V. Mikulec, and M. G. Bawendi, "The Band Edge Luminescence of Surface Modified CdSe Nanocrystallites: Probing the Luminescing State," *J. Chem. Phys.* **106**(23), 9869–9882 (1997).

12. A. Schroedter, H. Weller, R. Eritja, W. E. Ford, and J. M. Wessels, "Biofunctionalization of silica-coated CdTe and gold nanocrystals," *Nano Lett.* **2**(12), 1363–1367 (2002).
13. T. Pellegrino, L. Manna, S. Kudera, T. Liedl, D. Koktysh, A. L. Rogach, S. Keller, J. Rädler, G. Natile, and W. J. Parak, "Hydrophobic nanocrystals coated with an amphiphilic polymer shell: a general route to water soluble nanocrystals," *Nano Lett.* **4**(4), 703–707 (2004).
14. B. Dubertret, P. Skourides, D. J. Norris, V. Noireaux, A. H. Brivanlou, and A. Libchaber, "In vivo imaging of quantum dots encapsulated in phospholipid micelles," *Science* **298**(5599), 1759–1762 (2002).
15. V. P. Torchilin, "Recent advances with liposomes as pharmaceutical carriers," *Nat. Rev. Drug Discov.* **4**(2), 145–160 (2005).
16. R. Generalov, S. Kavaliauskiene, S. Westrom, W. Chen, S. Kristensen, and P. Juzenas, "Entrapment in phospholipid vesicles quenches photoactivity of quantum dots," *Int. J. Nanomedicine* **6**, 1875–1888 (2011).
17. H. Cabrera, D. Korte, and M. Franko, "Mode-mismatched confocal thermal-lens microscope with collimated probe beam," *Rev. Sci. Instrum.* **86**(5), 053701 (2015).
18. R. A. Cruz, V. Pilla, and T. Catunda, "Quantum yield excitation spectrum (UV-visible) of CdSe/ZnS core-shell quantum dots by thermal lens spectrometry," *J. Appl. Phys.* **107**(8), 0835041 (2010).
19. H. Cabrera, F. Cordido, A. Velázquez, P. Moreno, E. Sira, and S. A. López-Rivera, "Measurement of the Soret coefficients in organic/water mixtures by thermal lens spectrometry," *C. R. Mec.* **341**(4-5), 372–377 (2013).
20. E. Marin, *Thermal Wave Physics and Related Photothermal Techniques: Basic Principles and Recent Developments* (Transworld Research, Kerala India, 2009), Chap. 1.
21. L. C. Malacarne, N. G. C. Astrath, A. N. Medina, L. S. Herculano, M. L. Baesso, P. R. B. Pedreira, J. Shen, Q. Wen, K. H. Michaelian, and C. Fairbridge, "Soret effect and photochemical reaction in liquids with laser-induced local heating," *Opt. Express* **19**(5), 4047–4058 (2011).
22. N. Arnaud and J. Georges, "On the analytical use of the Soret-enhanced thermal lens signal in aqueous solutions," *Anal. Chim. Acta* **445**(2), 239–244 (2001).
23. H. Cabrera, E. Sira, K. Rahn, and M. Garcia-Sucre, "A thermal lens model including the Soret effect," *Appl. Phys. Lett.* **94**(051103), 1–3 (2009).
24. A. D. Bangham, M. M. Standish, and J. C. Watkins, "Diffusion of univalent ions across the lamellae of swollen phospholipids," *J. Mol. Biol.* **13**(1), 238–252 (1965).
25. R. H. Müller, C. Jacobs, and O. Kayser, "Nanosuspensions as particulate drug formulations in therapy. rationale for development and what we can expect for the future," *Adv. Drug Deliv. Rev.* **47**(1), 3–19 (2001).
26. L. W. Zhang, C. J. Wen, S. A. Al-Suwayeh, T. C. Yen, and J. Y. Fang, "Cisplatin and quantum dots encapsulated in liposomes as multifunctional nanocarriers for theranostic use in brain and skin," *J. Nanopart. Res.* **14**(7), 882–899 (2012).
27. W. T. Al-Jamal, K. T. Al-Jamal, P. H. Bomans, P. M. Frederik, and K. Kostarelos, "Functionalized-quantum-dot-liposome hybrids as multimodal nanoparticles for cancer," *Small* **4**(9), 1406–1415 (2008).
28. D. Simberg, S. Weisman, Y. Talmon, and Y. Barenholz, "DOTAP (and other cationic lipids): chemistry, biophysics, and transfection," *Crit. Rev. Ther. Drug Carrier Syst.* **21**(4), 257–317 (2004).
29. G. Guo, W. Lin, J. Liang, Z. He, H. Xu, and X. Yang, "Probing the cytotoxicity of CdSe quantum dots with surface modification," *Mater. Lett.* **61**(8-9), 1641–1644 (2007).
30. R. A. Cruz, A. Marcano, C. Jacinto, and T. Catunda, "Ultrasensitive thermal lens spectroscopy of water," *Opt. Lett.* **34**(12), 1882–1884 (2009).

1. Introduction

Quantum dots (QDs) have shown promising properties for a variety of biomedical applications [1], in particular they are useful for in vivo cell labeling, imaging and detection [2]. In comparison to organic dyes and fluorescent proteins, QDs offer several unique advantages, such as size and composition dependent emission, large optical absorption coefficient, very high levels of brightness, a broad absorption spectrum, a narrow emission spectrum and high photo-stability. However QDs contain toxic components (e.g. Cd in the CdSe/ZnS system studied in this paper), which could be released and kill cells [3]. Consequently, their therapeutic application in a biological environment meets challenges in delivery to target cells and to specific intracellular sites. Additionally, they are hydrophobic in their native state and cannot be dissolved in aqueous media [4]. To increase the hydrophilicity, a wide variety of surface coatings have been applied, among them polyethylene glycol, proteins, polymers and amine or carboxyl functional groups [5,6]. This surface modification often leads to decreases in the QDs fluorescence intensity and photo-stability [7–11], which requires higher doses of administered QDs for in vivo applications increasing the potential toxicity. A direct way to neutralize the toxic effects of QDs is to encapsulate them to become biologically inert [12,13].

Liposomes, also called vesicles, constitute one of the clinically most established type of nanoparticle today, with an extensively investigated pharmacological profile for various therapeutic and diagnostic applications [14,15]. They consist on a lipid bilayer (hydrophobic

region) surrounding an aqueous phase (hydrophilic compartment) and can be engineered to carry different drug molecules of polar or apolar character. They offer a promising solution for QDs encapsulation to prevent cytotoxicity and are good vehicles for the transport of drugs. Additionally, their surface charge can be easily modified with established methodologies. Unfortunately, the encapsulation of quantum dots by liposomes further decreases their fluorescence lifetime and intensity. Generalov *et al* [16] postulated that fluorescence quenching could be attributed to the protein adsorption on the QDs' surface and the acidic environment, which produce a high density of defects on their surfaces, leading to loss of quantum yield. This quenching of the fluorescence limits the application of common methods used for measurement of the encapsulation efficiency of QDs by liposomes.

One of the main goals of the presented work is to solve the mentioned above problem by applying the recently developed thermal lens microscopy (TLM) for QDs characterization. The applied TLM technique is based on the counter propagating pump-probe beams [17] in the mode-mismatched optimized [18,19] thermal lens (TL) configuration. Due to the fluorescence quenching mentioned above, the non-radiative recombination mechanisms following light absorption become important. This fact makes the use of photothermal [20] characterization tools useful, in particular thermal lens based methods [18,19]. Malacarne *et al.* [21] reported a theoretical model and experimental results for laser-induced local heating in liquids, and proposed a method to detect and quantify the contributions of photochemical and Soret effects in several different situations. In fact, this situation may lead to erroneous interpretation of experimental results if only one effect is assumed to occur and if absolute values need to be determined [21]. However, the contribution of these effects to the total signal is less than 10-20% [22,23] and could be neglected in the case of non absolute measurements such as calibration curves for encapsulation efficiency determination and photostability quantification.

The case studied in the present research was carboxyl CdSe/ZnS (Q21321 MP, Qdot 655 ITK™) QDs, which have been encapsulated by phospholipids liposomes and whose size distribution was measured using both dynamic light scattering (DLS) and high resolution transmission electron microscopy (HRTEM). Using a TLM the encapsulation efficiencies of QDs by liposomes were determined. The cytotoxic activity against breast cancer line MDA-MB-231 cells was examined too.

2. Materials and methods

2.1 Sample preparation

CdSe/ZnS QDs encapsulated by phospholipids Liposomes (Lipodots) were prepared according to the procedure described in the literature [24]. It was based on dissolving soy lecithin and cholesterol (4:1 wt respectively) in an organic solvent, which was a mixture of chloroform and methanol (ratio 9:1 volume respectively). The mixture was stirred for 10 minutes with a magnetic stirrer at 350 rpm. Then, the organic solvents were rotated for 2 hours in a rotary evaporator (Yamato RE500) at a temperature of 37°C, a pressure of 25 cmHg and a speed of 50 rpm. As a result of evaporation a lipid film was obtained, which was hydrated using a solution of deionized water and propylene glycol (24:1 volume respectively) and gently stirred at 50 rpm for 2 hours. Meanwhile, QDs (Qdot 655 ITK, average size of ~8 nm) were added to the dispersion. They were purchased from Invitrogen Corp as 8 µM stock solutions in 50 mM borate buffer and further diluted in deionized and filtered water to necessary concentrations. QDs solutions (1.25, 2.5, 10, 20, 30, 40, 50 nM) were prepared from 5, 10, and 40 µl QDs standard stock solutions (in water) and mixed with liposomal complexes to obtain the adequate QDs concentration inside the liposomes.

The average hydrodynamic diameter of empty liposomes obtained by thin-film hydration, was in the range 100-300 nm and the average size of lipodots was ~250 nm. In order to reduce the size distribution the liposomal solution was sonicated (Ultrasonic Elma-D78224) for 5 minutes at 25 °C, 25 kHz and a 60% potency. To homogenize the size of the liposomal formulation the final solution was ultrafiltered through a 0.22 µm permeation membrane

(Pellicon XL device, Millipore). This process was performed several times until a clear solution was obtained. To get a uniform size of the liposomes, 21 passages were performed. The average size of lipodots decreased considerably from 250 to ~180 nm. Non-encapsulated QDs were removed by ultrafiltration at 4000 rpm (rotor radius 14 cm, centrifuge model 5804 R; Eppendorf AG, Hamburg, Germany) using a 200 nm Vivaspin 6 filter (Vivascience AG, Hannover, Germany). When not in use, the liposomes were stored in a refrigerator (6°C).

CdSe/ZnS working standard solutions in the range between 0.8 and 13 nM were prepared from stock solution by appropriate dilution with deionized and filtered water.

2.2 High resolution transmission electron microscopy

The nanoparticle structures and sizes were measured using HRTEM (MET JEOL JEM-2100 operating at 200 kV). One drop of plain lipodots was positioned on a copper grid with carbon film for forming a thin film specimen.

2.3 Size distribution and zeta potential

The size (hydrodynamic diameter) and distribution of empty liposomes and lipodots were determined by dynamic light scattering (DLS) technique (Nano Zeta sizer Malvern, ZEN 3600). The same technique was used to determine the zeta potential.

2.4 Thermal lens microscopy

To select the proper wavelength of the excitation pump ($\lambda = 405.0$ nm) and probe ($\lambda = 632.8$ nm) beams, the absorption spectra (measured by a Lambda 650 PerkinElmer) was recorded. As shown in Fig. 1 CdSe/ZnS QDs in water (500 nM) showed a broad light absorption spectrum with strong intensities in the blue region, which decrease considerably towards the red region.

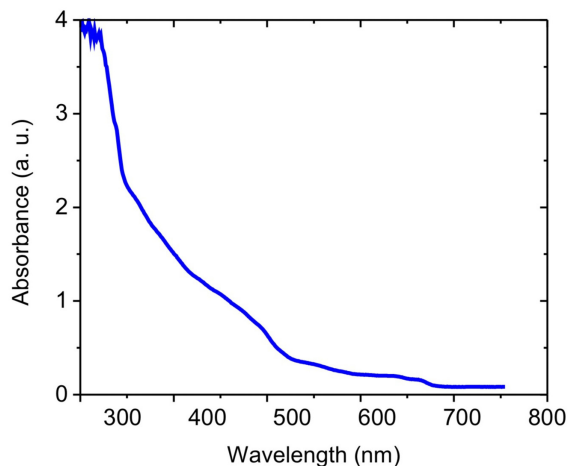


Fig. 1. UV-Vis. Absorption spectrum of 500 nM CdSe/ZnS QD655 QDs in water.

The scheme of the TLM set-up is shown in Fig. 2 [17]. The excitation and probe beams are counter propagating coaxially through the sample and the microscope objective lens. The Gaussian (TEM_{00}) 405 nm output wavelength excitation beam from a excitation laser diode (LASEVER LSR405ML-200) is electronically TTL modulated in intensity at a 50% duty-cycle. After reflected by a dichroic mirror, the excitation beam is focused by an inverted microscope objective (0.65 NA 40X, SP Nikon) onto a sample (0.4 mm quartz cuvette with QDs solutions). The sample is mounted onto a XYZ-translation stage (ThorLabs), which

allows to settle the optimal position and focus. The measured spot radius (by the use of a beam profiler Thorlabs BP209VIS) is $\omega_0 = 3 \mu\text{m}$. The pump beam power measured at the sample surface position is 20 mW. The probe beam laser is a 632.8 nm wavelength continuous He–Ne laser (JDS UNIPHASE). It is collimated ($\sim 4 \text{ mm}$ width) by a sets of two lenses. Its power is reduced to 1mW before passing through the sample in the region where the TL is created, thus avoiding undesirable heating. After that, it propagates through the inverted objective which in this way is also used as a condenser to form an image of the TL effect at the pinhole plane located in front of a detector photodiode (Thorlabs PDA36A, Si Switchable Gain Detector PD), which detects resulting probe beam intensity changes. Polarizers placed in front of both lasers eliminate rays coming back to the lasers cavity removing feedback or self-mixing effects. An interference filter placed in front of the detector allows only the probe beam to reach it. The TL signal registered by the photodiode is recovered using a lock-in amplifier (SR830 DSP from Stanford Research Systems) synchronized at the modulation frequency and its temporal evolution is visualized by a digital oscilloscope (BK Precision 2524).

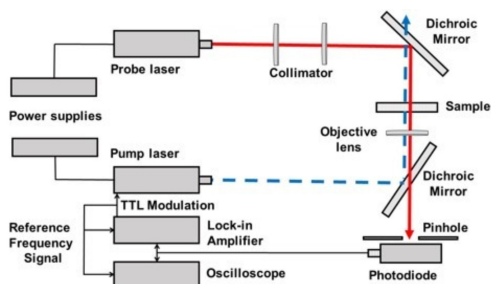


Fig. 2. TLM experimental setup.

This technique allows to perform the low concentration measurements [17], used in this paper, to determine the encapsulation efficiency of the QDs by liposomes. The methodology consists in measuring the PT signal amplitude as a function of known QDs concentrations in water, i.e. the calibration curve. Then the unknown concentration of QDs in liposomes is determined using the calibration curve. Then, the conversion efficiency can be calculated as the ratio of the QDs concentration inside liposomes and the initial concentration of QDs mixed with the empty liposomes solution.

2.5. Cytotoxicity in tumor cells by lipodots

Breast cancer cells MDA-MB-231 were cultured in plates of 25 cm². After culturing they were placed in an incubator (brand Binder C 150 UL) at 37 °C and 5% CO₂. Once they reached a 100% confluence, the cells were counted and 96-well plates were seeded with 7000 cells per well, which were incubated at 37 °C and 5% CO₂. After 24 hours, empty liposomes and lipodots with different concentrations of quantum dots (0.45, 0.69, 1.17, 1.4, 2.28, 2.41, 3.6, 7.0 and 13.3 nM) were placed in the cell culture. The cell viability was analyzed by the MTT technique (Thiazolyl Blue Tetrazolium Bromide) at 24, 48 and 72 h. Evaluations were performed in triplicate.

3. Results and discussion

3.1 Size distribution and z potential

HRTEM microphotographs show that lipodots are mainly multilamellar vesicles of variable sizes between 100 and 200 nm with an average value of 180 nm, which correlate well with the values determined by the light scattering method. Figure 3 show the QDs (dark spots) encapsulated into the liposomes or their membranes, indicating an efficient loading.

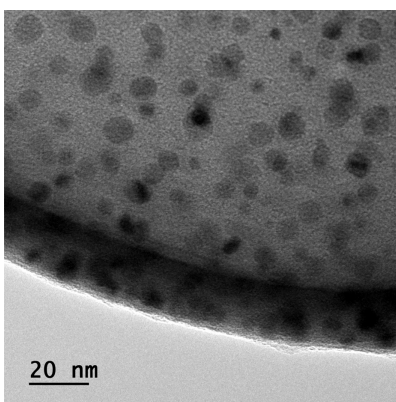


Fig. 3. HR-TEM micrographs of the CdSe/ZnSe QDs encapsulated by the liposome complexes (lipodots).

The vesicles size and z potential are summarized in Table 1. Dynamic light scattering measurements show that the average size of the liposomes was ~ 142.3 nm. QDs loading produced an increase to about 180 nm. This corresponds practically to the size determined by HRTEM.

Zeta potential measurements show that the surface potential of empty liposomes is negatively charged at approximately -32.7 mV. The zeta potential is an indicator of the stability of nanocarriers. A physically stable nanocarrier simply stabilized by electrostatic repulsion should have a minimum zeta potential of ± 30 mV [25]. Therefore, most of the dispersions prepared in this study were stable enough. The loading of QDs reduces the negative zeta potential to -13.1 mV, which is a value similar to other reported in literature [26]. Additionally, the presence of nonionic materials in the liposomal bilayers may shield the surface potentials. The significant change in the zeta potential (from -32.7 to -13.6 mV), after QD encapsulation, indicates that, they are also located in the liposome bilayers (see Fig. 3) [26].

The positive surface charge is an essential issue responsible for increased cellular liposome uptake [4,27]. Lipodots used in this study possess a negative charge, what favors its bioimaging applications, since cationic surfactants and lipids (in general positive charged components) could cause cell damage [28,29].

Table 1. Size and z potentials for empty liposomes and lipodots

	D (nm)	St. Dev.	Z (mV)	St. Dev.
Liposomes	142.3	7.4	-32.7	4.0
Lipodots	180.0	8.0	-13.6	1.7

The increase in lipodot sizes (180 nm), comparing to empty liposomes (142.3 nm), may be the result of coupling the QDs within both, the phospholipid bilayers inside the outer membrane and in the aqueous region (Fig. 3).

3.2 TL measurements

Measurements of the TL signal for known concentrations of QDs in water were performed to construct the calibration curve shown in Fig. 4 and to determine the limit of detection (LOD) of the method. The pump beam power, P_e , was 20 mW and the modulation frequency was 5 Hz. Each point (red circles) in the curve corresponds to an averaging value of six independent measurements. As expected, the TL signal increases linearly with the increase in QDs concentration in the water solution. The QDs signal is distinguishable from background (empty liposomes in aqueous solution) down to a concentration as low as 0.5 nM.

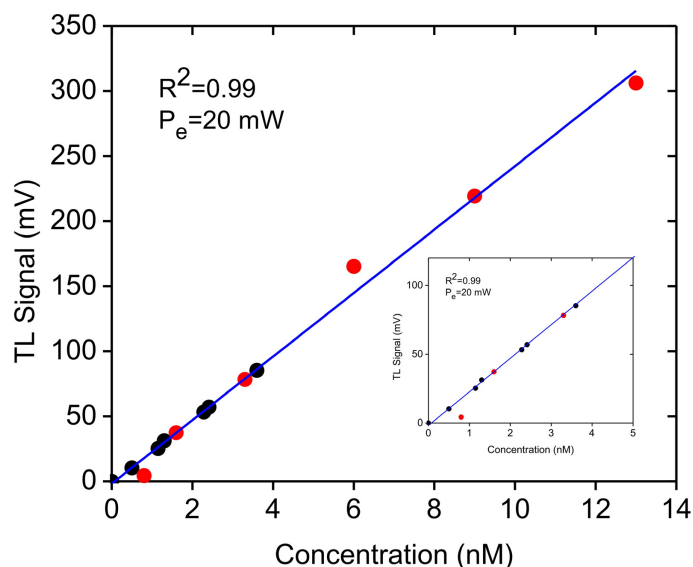


Fig. 4. Calibration curve describing the TL intensity as a function of QDs concentration in aqueous solution 0 to 13 nM. The solid line represents a result of a best least squares linear fit with $R^2 = 0.99$. Red circles correspond to measurements for QDs in water (without liposomes) and the black circles correspond to measurements for lipodots (QDs inside liposomes). The inset shows the curve below 5nM concentration for better visualization.

In the next step, the evaluation of QDs encapsulation was performed by measurement different lipodot preparations. For that purpose QDs at stock concentration 1.25, 2.5, 10, 20, 30, 40, 50 nM were mixed with liposomes and, after processing and filtering, the TL signal for each solution was measured. The obtained values were introduced in the calibration curve (black circles), so that the concentration of the analyzed species can be determined by interpolation, being in the range between 0.45 to 3.60 nM. The LOD was calculated as the three-fold standard deviation TLM signal of the empty liposomes in water divided by the slope of the calibration curve. The obtained value was $\text{LOD} = (0.13 \pm 0.02)$ nM and is related to the minimal signal achieved for lipodots which can be still distinguishable from the blank (empty liposomes in water). Recently, Cruz *et al.* [30] demonstrated a minimum absorption value of water between 360 and 400 nm and we have used a 405 nm excitation wavelength. Consequently, the LOD could be further reduced using lower excitation wavelength and higher excitation powers. As described above, the conversion efficiency is then calculated for each point as the ratio of the QDs concentration achieved inside liposomes (lipodots) and the initial concentration of QDs mixed with liposomes.

In Fig. 5, the encapsulation efficiency versus the initial concentration of QDs mixed with liposomes is shown. The optimum encapsulation efficiency is 36% at the lowest concentration, which is close to the value reported in literature [26], and decreases with increase in the concentration until a saturation tendency is achieved around a value of 7%. It must be remarked, that this efficiency is related only to the encapsulation of QDs with sizes smaller than 220 nm by the liposomes, because bigger QDs were filtered out during the preparation process as described above, which means, that the real encapsulation efficiency is even higher. This result suggests an optimum quantity of initial solution of QDs to be mixed with liposomes and a range between 1.25 and 10 nM seems to be reasonable. We hypothesize, that this result could be related to an optimum quantity of the initial concentration of QDs mixed with liposomes and to the fact, that there exists a limited place inside liposomes to be occupied by QDs. As a definition, the encapsulation efficiency is the ratio of QDs inside

lipodots divided by the initial concentration of QDs mixed with liposomes; therefore our technique not only determine the encapsulation efficiency but also the optimum quantity of the initial concentration of QDs to be mixed with liposomes.

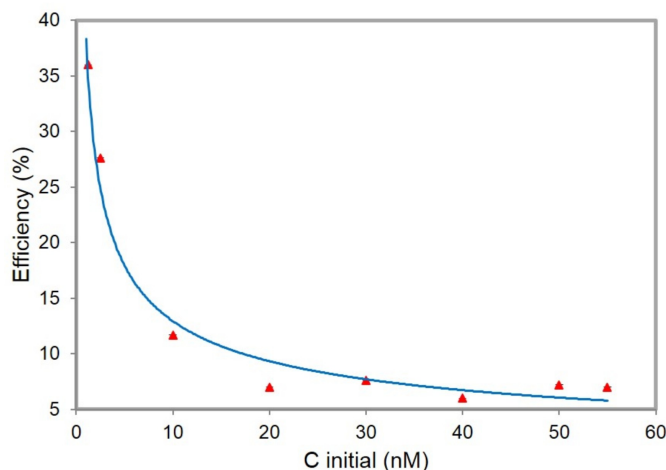


Fig. 5. Encapsulation efficiency as a function of the initial concentration of QDs mixed with empty liposomes. The solid line is only for visualization purposes.

Finally, to test the photo-stability of the samples under long time exposure (e.g. 40 minutes) to the excitation light beam, experiments were performed using a typical sample (3.6 nM of lipodots). Figure 6(a) shows the temporal evolution of the TL signal recorded at 5 Hz during 40 minutes excitation for the examined sample. As shown in Fig. 6(b), the peak to peak TLM signal remains almost constant over the time exposure, indicating that there is not photobleaching and that the lipodots system is photostable.

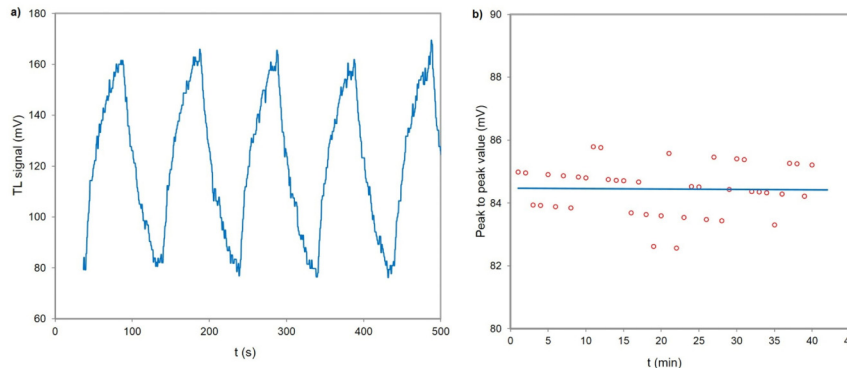


Fig. 6. (a) Temporal evolution of the TL signal at 5 Hz and (b) its peak to peak value during 40 minutes excitation for 3.6 nM lipodots. The solid line represents the mean of the peak to peak values.

3.3 Cytotoxicity

Since the application of functionalized lipodots is mainly in bioimaging, it is necessary to examine the cell viability at specific concentrations. Thus, experiments were carried out to apply different lipodot concentrations into the cell culture. In Fig. 7(a), it is shown the cell viability of the lipodots system for concentrations 0.41 to 3.3 nM, after applying to the MDA-MB-231 cancer cells line. A percent of cellular reduction, during 24 hours, was estimated between 5 and 10%, whereas for 72 hours it was between 10 and 18%, depending on the

lipodots concentration. When pure QDs were introduced, the effect was significantly reduced. This is an important information, in the case of the use of lipodots as biomarkers for in vivo imaging. Figure 7(b) shows, that when the concentration increases in the range between 1.7 nM and 13 nM, there are not significant differences in the cell viability for both lipodots and empty liposomes.

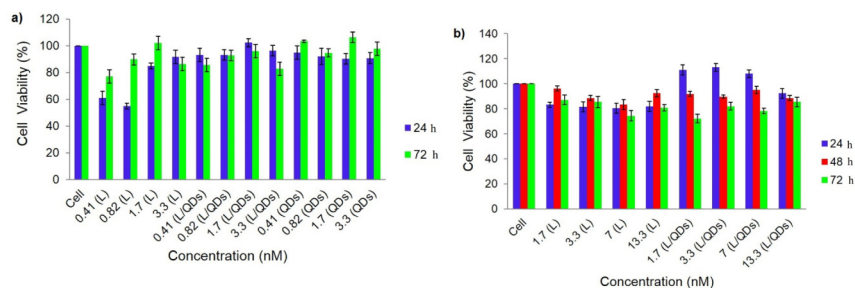


Fig. 7. Cellular viability on MDA-MB-231 line cancer cells for concentrations (a) 0.41 nM to 3.3 nM. L (empty liposomes), L/QDs (lipodots) and QDs (quantum dots), (b) 1.7 nM to 13.3 nM.

4. Conclusions

In this work QDs were successfully encapsulated by phospholipids liposome complexes with maximum encapsulation efficiency of 36%. HRTEM demonstrates, that QDs were mainly located in its aqueous central region, although some in liposomal phospholipid bilayers (membranes). The obtained solutions were biocompatible and could be dispersed in aqueous phase. The TLM method showed, that QDs located inside liposome complexes can be successfully detected. The LOD of presented method was 0.13 nM. The results of TL experiments showed, that lipodots present high photothermal conversion efficiency and excellent photostability. Dark toxicity study demonstrated, that at low concentrations (1–13 nM), the CdSe/ZnS QDs were not cytotoxic to the cell line used in this study.

Acknowledgments

This work was partially supported by CONACyT, by research grants from SIP-IPN 1638 and 20150390, and COFAA-IPN through the SIBE Program. H.C. gratefully acknowledges the financial support for a Sabbatical Stay at CICATA, IPN under grant 017/2014 from Centro Latinoamericano de Física, CLAF, and Secretaría de Ciencia, Tecnología e Innovación del Distrito Federal, México, and ICTP through the Research Associateship Program and SPIE-ICTP Anchor Research Laboratory. The authors also acknowledge the HRTEM facilities at CNMN-IPN.